Kinematic and Kinetostatic Synthesis of Planar Coupled Serial Chain Mechanisms

Venkat Krovi[†]
e-mail: vkrovi@eng.buffalo.edu

G. K. Ananthasuresh
e-mail: gksuresh@grip.cis.upenn.edu

Vijay Kumar
e-mail: kumar@grip.cis.upenn.edu

Mechanical Engineering and Applied Mechanics,
University of Pennsylvania,
Room 301C, GRASP Lab,
3401 Walnut Street,
Philadelphia, PA 19104

Single Degree-of-freedom Coupled Serial Chain (SDCSC) mechanisms form a novel class of modular and compact mechanisms with a single degree-of-freedom, suitable for a number of manipulation tasks. Such SDCSC mechanisms take advantage of the hardware constraints between the articulations of a serial-chain linkage, created using gear-trains or belt/pulley drives, to guide the end-effector motions and forces. In this paper, we examine the dimensional synthesis of such SDCSC mechanisms to perform desired planar manipulation tasks, taking into account task specifications on both end-effector motions and forces. Our solution approach combines precision point synthesis with optimization to realize optimal mechanisms, which satisfy the design specifications exactly at the selected precision points and approximate them in the least-squares sense elsewhere along a specified trajectory. The designed mechanisms can guide a rigid body through several positions while supporting arbitrarily specified external loads. Furthermore, torsional springs are added at the joints to reduce the overall actuation requirements and to enhance the task performance. Examples from the kinematic and the kinetostatic synthesis of planar SDCSC mechanisms are presented to highlight the benefits.
[DOI: 10.1115/1.1464563]

1 Introduction

Typical manipulation tasks require specification of the motion of the manipulated object as well as its force interactions with the environment. Further, many such tasks are inherently single degree-of-freedom (d.o.f.), parameterizable by a single variable such as the arc-length parameter. Hence, we introduce a novel configuration called *Single Degree-of-freedom Coupled Serial Chain* (SDCSC) mechanisms for executing such single degree-of-freedom manipulation tasks.

A variety of closed-loop mechanisms and general-purpose serial chain manipulators have been used in the past to accomplish such manipulation tasks. Four-bar linkages, such as the one shown in Fig. 1(*a*), can generate a wide variety of the desired trajectories using a single actuator but tend to be unsuitable for cluttered environments due to the interference of the links with each other and with the environment. Serial chain manipulator configurations, such as the one shown in Fig. 1(*b*), are therefore preferred in cluttered environments but require multiple articulations (and hence actuators) and coordinated control. Constraints need to be created between the joint articulations, in software, to accomplish the single degree-of-freedom manipulation tasks. While, the software reconfigurability of the constraints offers considerable flexibility, it comes at the price of increased complexity of actuation, coordination and control, especially for specialized or repetitive tasks. Tendon-driven serial-chain manipulators, such as the one shown in Fig. 1(*c*), permit the relocation of the actuators to the base of the manipulator, thereby reducing the inertia of the moving parts, but still require at least as many actuators as degrees of freedom.

SDCSC mechanisms are proposed here as an alternative to both closed-loop and serial chain linkages. Such mechanisms may be constructed by mechanically coupling the rotations of the links of an *n*-link, *n*-d.o.f. serial chain manipulator using cable and pulley drives or by gear-trains. Each coupling between two successive

joint rotations reduces one degree-of-freedom and repeated coupling reduces the overall degrees of freedom of the manipulator to one, as shown in Fig. 1(*d*). The resulting SDCSC mechanisms combine the simplicity of single-degree-of-freedom control and rigidity/strength afforded by closed-loop linkages with the modularity, compactness and reduced interference of serial chains. SDCSC mechanisms can be used to realize a range of end-effector trajectories using just one degree of freedom. Trajectories of increasing complexity and variety may be generated by increasing the number of links of the SDCSC mechanism, as illustrated in Fig. 2. In this paper, our interest is in developing dimensional synthesis tools to aid the design of SDCSC mechanisms for desired manipulation tasks.

Our work is motivated by the design of customized rehabilitation aids for the disabled [1]. The design requirement is for creation of passive articulated manipulators, which can be actuated by alternate functional body parts of the user (e.g., legs for hand amputees or head for quadriplegics) to realize a set of motions and forces. The passivity of mechanical constraint implementation, reduced interference with the environment, simplicity of control and low cost favor the use of the SDCSC configuration for such tasks. Figure 3(*a*) shows the fabricated prototype of a feeding mechanism, which powered solely by the motions of the quadriplegic user's head, permits the user to feed independently. This feeder features a SDCSC type manipulator in the sagittal plane and in this paper, we will examine the shaping of the end-effector motion and input torque profile in the examples.

Some of the above discussed benefits also make such SDCSC configurations attractive for use in assembly tasks in manufacturing plants, either as a low cost solution automation solution or to work in cooperation with the human operator. Further, the design may be enhanced easily by permitting all the principal structural parameters for a given SDCSC manipulator, such as link lengths, coupling ratios and initial posture, to be adjustable. Figure 3(*b*) depicts an industrial application of such a reconfigurable manipulation assist device, where the end-effector forms a passive virtual guide rail to constrain and redirect the motions and forces of the user to the prescribed task-space curve while retaining the ability to be reconfigured to realize other constrained motions [2].

Finally, the kinetostatic design and optimization methods pre-
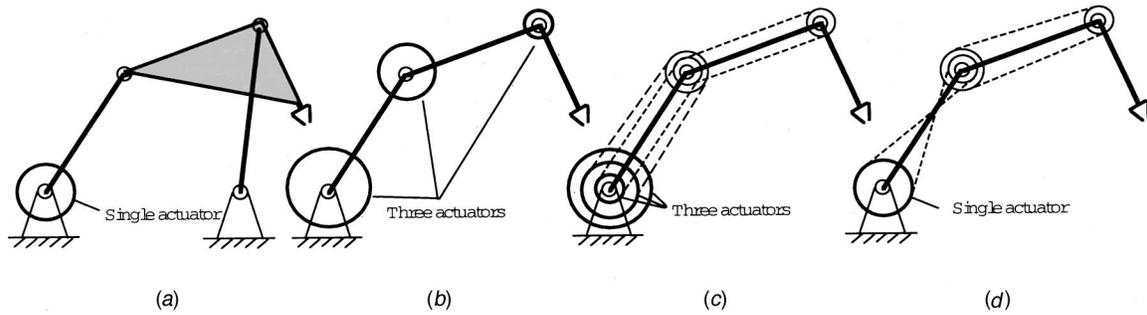

Fig. 1 Different mechanism configurations: (*a*) **single degree-of-freedom four-bar linkage;** (*b*) **multi-degree-of-freedom conventional, serial-chain linkage;** (*c*) **tendon-driven serial chain linkage; and** (*d*) **single-degree-of-freedom coupled serial chain mechanism.**

sented in this paper can also be readily applied to the design of shaped motion and force profiles with applications in diverse arenas ranging from the design of exercise and rehabilitation equipment [3] to the design of compliant mechanisms [4].

The organization of the rest of this paper is as follows: In Section 2, we present a short review of literature of mechanisms designed with hardware couplings between joints and briefly survey relevant kinematic and force-measure based synthesis methods. Other references are included, as appropriate, in subsequent sections. In Section 3, we present the design synthesis framework used to realize optimal mechanisms which satisfy the design specifications exactly at the selected precision points and in the least-squares sense elsewhere. In Section 4, we apply this frame-

work for matching desired *kinematic specifications* on the end-effector, typical of rigid body guidance (RBG) and path following (PF) tasks. However, in other applications, the force interactions between the manipulator and its environment need to be taken into account. Hence, in Section 5, the design process is enhanced to permit the design of mechanisms that can guide a rigid body through several positions while supporting arbitrarily specified external loads using a judicious combination of motion, structural equilibration and actuation. Spring assists are also considered to reduce the overall actuation requirements. Section 6 concludes the paper.

2 Related Work

As noted in the previous section, the coupling between joint rotations of a multi-d.o.f manipulator can be done in software or in hardware. Such software coupling of the joint rotations to specific mode shapes, has been employed in the past for efficient inverse kinematic computation and gait generation of hyperredundant manipulators and vehicles [5]. In our work, however, we employ hardware components, such as gear-trains or cable-pulley drives, to realize a linear coupling between the articulations.

Many instances of the use of mechanical couplings between articulations exist in the literature. An excellent summary of geared and belted mechanisms is provided by Hunt [6], p. 235 who states "there is no limit to the possible arrangements when gears and bands are used especially for non-circular gears or band wrapping profiles." Thus, mechanical couplings can provide a flexibility paralleling the algorithmic method of coupling joint ro-
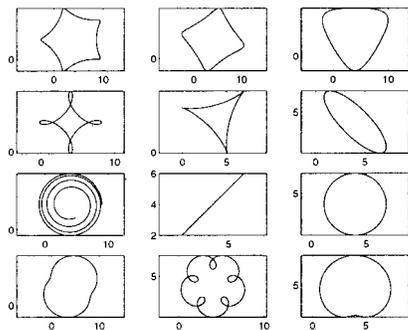

Fig. 2 Typical end effector paths for a single-degree-of-freedom, coupled, serial-chain mechanism
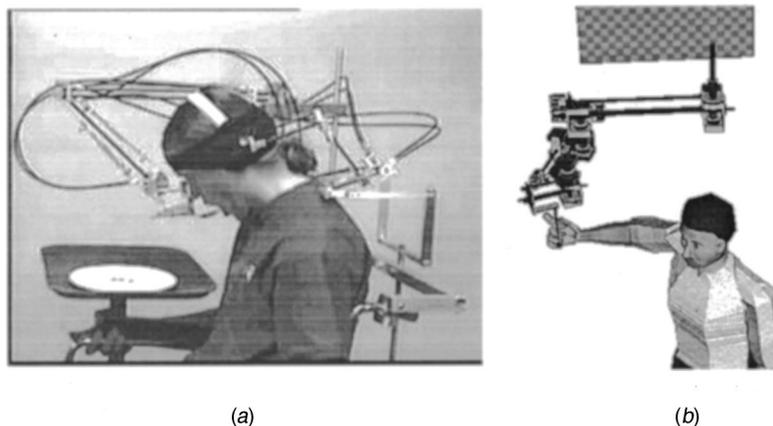

Fig. 3 (*a*) **Head controlled feeding telethesis (featuring the Coupled Serial Chain configuration).** (*b*) **Use as a passive manipulation assist "guide rail" in an industrial setting.**

tations, along with the additional benefits of high precision, backlash free and low friction operation when taut steel bands are used. The cycloid crank was developed as an extension of the R-R crank, by replacing the revolute joints with gear-pairs, for use in studying mechanisms like the geared 5-bar [7]. Sandor [8] developed the ''Cycloidal Burmester Theory'' for use in the synthesis of cycloid cranks to reach the maximum number of precision points. However, further extensions to the cycloidal point theory for synthesis were never pursued with the notable exception of the Bicycloidal crank [9].

Tendon-driven serial-chain manipulators have been studied extensively but primarily from the viewpoint of full control of an n-d.o.f. manipulator. See Tsai [10] for a good review. The SDCSC configuration shows an apparent similarity to tendon-driven manipulators and in particular, the soft gripper mechanism and the Coupled-Tendon Arm developed by Hirose. The soft gripper [11] is a snake-like tendon driven mechanism which can adapt its shape to the perimeter of an arbitrarily shaped object while creating a uniform grasping force on all the gripper surfaces. In contrast, the cables and pulleys in the SDCSC configuration create a rigid coupling between the joint rotations which predetermines the shape of the manipulator for a given base-joint rotation. Further, the Coupled-Tendon Arm [12] is a multi-d.o.f. tendon driven manipulator where the emphasis is on the use the coupled tendons to permit an even distribution of the actuation power requirements among the multiple actuators, as opposed to the single d.o.f. actuation achieved in the SDCSC configuration.

Fewer examples of the use of tendon-drive actuation to reduce the degrees of freedom/actuators exist. In terms of antiquity, Leonardo Da Vinci is believed to have created an iron man with an elaborate system of cable and pulley drives to move the arms and legs using a single water wheel [13]. In more recent times, tendon-drives have been used to reduce the degrees of freedom of anthropomorphic finger mechanisms, such as in the three-jointed two-degree-of-freedom finger [14] or the three-jointed single-degree-of-freedom finger [15]. While past mechanisms may have been designed by trial and error [13] or analysis [14,15], in the subsequent sections we will focus on determination of the dimensions of the device to satisfy a set of design specifications by *synthesis*.

A wealth of literature exists for synthesis of mechanisms to meet kinematic design requirements and the reader is referred to standard texts such as[16] for more details. In contrast, the synthesis of mechanisms to match force- or energy-related design criteria has received lesser attention. Examples of such criteria include: prescribed mechanical advantage; prescribed input-output force characteristics; as prescribed energy levels. Such force-measures have been included as design constraints to be satisfied

explicitly at precision points as well as in objective functions to be optimized over a range. In many cases, specifying the force measure was shown to be equivalent to specifying kinematic relationships by way of the principle of virtual work. Bagci [17] presented methods for synthesis of linkages by specifying the mechanical advantage at each PP, or specifying the mechanical advantage over a range. Matthew and Tesar [18] extended the finite position synthesis to infinitesimally separated motion synthesis to facilitate the specification of the input force histories. Idlani et al. [19] developed a dimensional synthesis technique to determine the mechanism and spring parameters of mechanisms with specified elastic (and total) potential energy at precision points.

Even more recent, is the development of the *kinetostatic synthesis approach*, permitting the satisfaction of both force-measure and kinematic design criteria simultaneously. Huang and Roth [20] formulated and solved kinematic and force-measure design constraints at precision points simultaneously to synthesize closed-loop mechanisms, like the four-bar. Howell and Midha [4] solved similar sets of equations, for four-bar and slider-crank linkages with torsional springs at the joints, and identify three cases—decoupled, weakly-coupled and strongly-coupled—based on the extent of coupling between the variables of the kinematic and force-measure equations. These aspects will be discussed in greater detail in Section 5.

3 Design Methodology

Design specifications are typically presented as a set of desired positions and orientations on the end-effector and/or prescribed force interactions with the environment, to be matched or approximated as closely as possible. Precision Point Synthesis (PPS) and Optimization are two methods of mechanism design most commonly employed to determine the parameters of the mechanism that can satisfy these desired specifications.

The requirement to match design specifications exactly at Precision Points (PPs) creates constraints between the various parameters of the mechanism. The simultaneous solution of the resulting set of algebraic constraints is used to determine the parameters of the designed device. While exact matching of design specifications at greatest number of precision points is desirable, a limit on the maximum number of constraints is soon reached. Further, a simultaneous solution of the non-linear set of constraints is also required which restricts the usefulness of the PPS approach.

Several approaches address this limitation of small number of design specifications: the *Approximate Synthesis* approach [21] creates a least-squares/mini-max scheme for solving an overdeter-
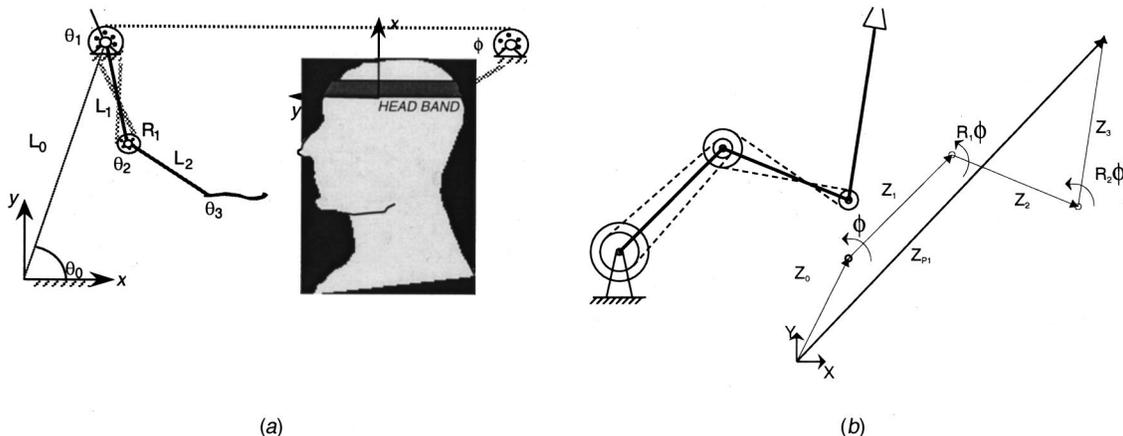

(a)   (b)

Fig. 4 (*a*) Schematic of operation of the head-controlled feeding device. (*b*) Physical and mathematical models of a 2-link SDCSC mechanism.

mined system of design specifications in the "best way"; the *Selective Precision Synthesis* approach [22] permits a region of variability around each design specification to enable inclusion of more design specifications; and the *incomplete specification* [23] or *mixed specification* [24] approaches advocate prioritization among the design specifications at precision points. The generalization of the least-squares specification matching is the formulation of an optimization problem with a suitable least-squares objective function which is minimized over the complete set of parameters of the mechanism. The resulting mechanism would then satisfy *all* the desired specifications in the least squares sense without guaranteeing an exact matching of *any* specification.

In this paper, we combine the benefits of precision point synthesis and optimization. A constrained optimization problem is created by introducing a small number of design constraints for exact specification matching. Solving these constraints, we obtain an explicit linear solution for the independent parameters in terms of certain dependent parameters. An optimization is performed over the set of independent parameters to obtain the dimensions of the optimal mechanism. The benefits include addition of structure to the problem while permitting adequate flexibility/choices to the designer; reduction of dimension of the overall optimization problem; and the ability to match at least some of the design specifications exactly.

Examples. The design of a head-controlled feeding device, Fig. 4(*a*), will serve as the primary example. This feeding device has to be synthesized to take an end effector (feeding utensil) from the plate and mouth while carrying an end-effector load (food) in a smooth single parameter motion. Currently, the weight of the links and friction at the joints is not modeled. The position of the mouth and the position of the plate are typically chosen as precision points with typical load values attributable to the weight of the food. In the subsequent two sections, we examine the kinematic and kinetostatic synthesis of two- and three-link SDCSC mechanisms that can perform the feeding task. We also explore the minimization of the input torque requirements by a combination of structural equilibration and spring assists. This is critical in our case since the feeding device is to be powered by motions of the user's body parts with limited permissible ranges of motions and forces.

4 Planar Kinematic Design and Optimization

4.1 Precision Point Synthesis. The loop-closure equations for the end effector of an *N*-link SDCSC mechanism (shown schematically in Fig. 4(*b*)) can be written as a function of ϕ, the *input link rotation angle relative to the first position* as:

$$Z_P(\phi) = Z_0 + Z_1 e^{i\phi} + Z_2 e^{iR_1\phi} + \ldots + Z_N e^{iR_{(N-1)}\phi}$$

$$= L_0 e^{i\theta_0} + L_1 e^{i\theta_1} e^{i\phi} + L_2 e^{(i\theta_2} e^{iR_1\phi)} + \ldots$$

$$+ L_N e^{i\theta_N + iR_{(N-1)}\phi} \tag{1}$$

$$\Theta(\phi) = \angle Z_N + R_{(N-1)}\phi \tag{2}$$

where the kth link may be written as $Z_k = Z_{kx} + iZ_{ky} = L_k e^{i\theta_k}$, $L_k = |Z_k|$, $\theta_k = \angle(Z_k)$ and $e^{i\psi} = \cos(\psi) + i\sin(\psi)$ and Θ is the final orientation of the end effector.

The kinematic design constraints are obtained by evaluating Eqs. (1) and (2) at the *M precision points (PP)* on the trajectory (indexed by $1 \leq j \leq M$). These design constraint equations may be rewritten in a compact matrix form as shown below:

$$Z_0 = P_1 - (Z_1 + Z_2 + \cdots + Z_N)$$

$$\begin{bmatrix} \Delta P_2 \\ \Delta P_3 \\ . \\ \Delta P_M \end{bmatrix} = \begin{bmatrix} e^{i\phi_2}-1 & e^{iR_1\phi_2}-1 & \cdots & e^{iR_{N-1}\phi_2}-1 \\ e^{i\phi_3}-1 & e^{iR_1\phi_3}-1 & \cdots & e^{iR_{N-1}\phi_3}-1 \\ . & & . & \\ e^{i\phi_M}-1 & e^{iR_1\phi_M}-1 & \cdots & e^{iR_{N-1}\phi_M}-1 \end{bmatrix}$$

$$\times \begin{bmatrix} Z_1 \\ Z_2 \\ . \\ Z_N \end{bmatrix}$$

$$\tag{3}$$

$$\begin{bmatrix} \Delta\Theta_2 \\ \Delta\Theta_3 \\ . \\ \Delta\Theta_M \end{bmatrix} = R_{(N-1)} \begin{bmatrix} \phi_2 \\ \phi_3 \\ . \\ \phi_M \end{bmatrix}$$

where $\Delta P_M = P_M - P_1$ and $\Delta\Theta_M = \Theta_M - \Theta_1$.

The orientation constraint equation is not required for the *Path Following (PF)* problem and is identically satisfied at the first position ($\phi_1 = 0$) in the *Rigid Body Guidance (RBG)* problem.

Table 1 Determination of the maximum feasible number of precision points for an *N*-link, SDCSC mechanism for the *RBG* and *PF* problems

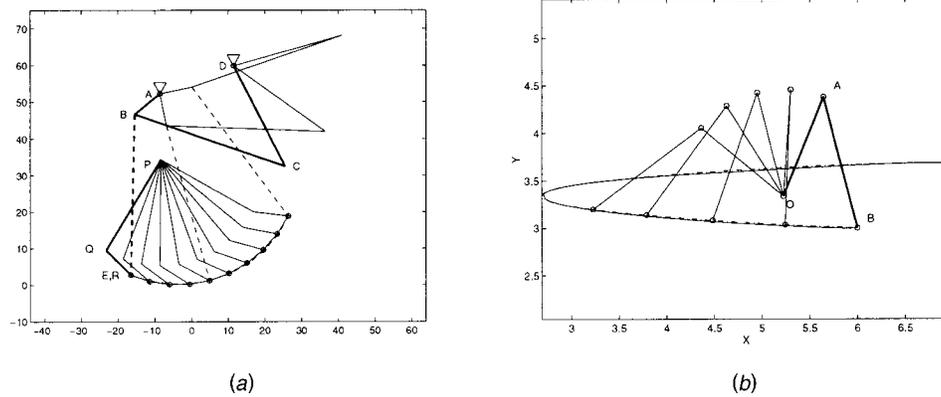|	RBG Problem				PF Problem			
Links	Equations	Variables	Free Choices	Max M	Equations	Variables	Free Choices	Max M
N	$3M-1$	$3N+M$	$3N+1-2M$	$M \leq \lfloor \frac{3N+1}{2} \rfloor$	$2M$	$3N+M$	$3N-M$	$M \leq 3N$
2	$3M-1$	$6+M$	$7-2M$	$M \leq 3$	$2M$	$6+M$	$6-M$	$M \leq 6$
3	$3M-1$	$9+M$	$10-2M$	$M \leq 5$	$2M$	$9+M$	$9-M$	$M \leq 9$
4	$3M-1$	$12+M$	$13-2M$	$M \leq 6$	$2M$	$12+M$	$12-M$	$M \leq 12$
5	$3M-1$	$15+M$	$16-2M$	$M \leq 8$	$2M$	$15+M$	$15-M$	$M \leq 15$

Fig. 5 Dimensional Synthesis solutions: (*a*) Sample SDCSC mechanism and 4-bar linkage solutions for an *RBG* problem. (*b*) Sample SDCSC mechanism tracing an elliptical shape for a *PF* problem.

Note that the end-effector position constraints are linear in the unknowns Z_j but not the unknowns R_j or ϕ_k and that the orientation constraints are linear in the unknowns ϕ_k. In the RBG case, we select the $N-1$ unknowns $(R_1 \ldots R_{(N-1)})$ to form the set of independent variables. This permits us to solve the orientation constraints linearly to determine the $M-1$ input crank angles, $\phi_2 \ldots \phi_M$ and subsequently the position constraints linearly to obtain the Z_j. In the PF case, we specify $N-1$ unknowns $(R_1 \ldots R_{(N-1)})$ and the $M-1$ input link rotation angles $(\phi_2 \ldots \phi_M)$ as the independent variables and solve for the remaining dependent variables Z_j using the position constraint equations.

In addition to suitable partitioning, the linear solution for the dependent variables will only be feasible if the number of independent variables is less than the number of available free choices available at any given time (see Table 1). This requirement limits the maximum number of precision points which will still permit a linear solution of the synthesis equations as shown below:

$$
\begin{array}{ccccccc}
& \overline{RBG} & & & & \overline{PF} & \\
N-1 & \leqslant & 3N+1-2M & & N+M-2 & \leqslant & 3N-M \\
M & \leqslant & N+1 & & M & \leqslant & N+1
\end{array}
$$

$$(4)$$

4.2 Optimization. Typically, the design specifications are presented as a discrete set of end-effector positions, orientations and/or forces. Interpolatory cubic splines are employed to obtain the corresponding C^2 continuous desired specification "curves." The optimization scheme is developed by selecting a suitable objective function to minimize and employing the free choices (independent variables) as optimization variables.

The objective function must be a measure of the discrepancy between the *desired* specification and *generated* curves. The generated curve is the one realized by the mechanism synthesized using the precision point synthesis equations. The *structural error* [16], computed as the sum of the squares of the discrepancy of the two curves evaluated at pairs of *correspondence points*, is employed here. Two approaches for the identification of the correspondence points are presented below.

Orientation Matching Correspondence. In the RBG problem the objective function is required to reflect the discrepancy between the desired and generated end-effector orientations as well as positions. Most schemes consider the explicit combination of

the orientation and position errors into an inhomogenous objective function which depends on the choice of a length scale. While some approaches seek to eliminate the inhomogeneity of units and the trigonometric non-linearity [25], the objective function still depends on "non-vanishing representative length" units. In our approach, we parameterize each curve using the orientation. Orientation matching correspondence is created by first finding the input link rotation angle (ϕ) of the generated mechanism to match the desired orientation using Eq. (2). The position of the (orientation matching) correspondence point is then determined using the forward kinematics equations for this input link rotation angle. This eliminates the explicit inclusion of the orientation discrepancy in the objective function.

Equal Arc-Length Segment Correspondence. In the path following problem, the lack of orientation information necessitates a new scheme to obtain the correspondence points. The parametric arc-length is obtained by chordal approximation of a finely discretized set of points for each curve. Each curve can then be divided into N equal segments based on the arc-length. The endpoints of each segment (on the two curves) form the two sets of points that have a one-to-one correspondence to each other based on the arc-length measure. The structural error with equal-arc length correspondence points accurately assesses the extent of discrepancy and that convergence to the correct solution is rapid and is discussed further in [26].

Implementation Details. We implement the optimization scheme in MATLAB using the *constr( )* function, provided in the Optimization Toolbox, for the constrained non-linear optimization. The routine is based on a sequential quadratic programming method with BFGS Hessian updates of the Lagrangian at each iteration. Auxiliary constraints are applied to the problem by appending them to the objective by way of Lagrange multipliers. These include upper and lower bounds on the mechanism parameters and order constraints on the input crank angle to ensure that $\phi_j < \phi_{(j+1)}$. In the examples discussed below, all problems converged to the depicted solutions in typically under a minute on a 500 MHz PC running MATLAB. Multiple solutions are possible due to the nonlinearity and non-convexity, which is typical in mechanism optimization-based synthesis problems. The optimum solution is dependent on the initial guess assigned to the design variables and the optimal solutions do not necessarily represent a global minimum. However, as demonstrated, the combination of precision point synthesis and optimization over the free choice variables gives a solution within the feasible region that closely matches the desired specifications.
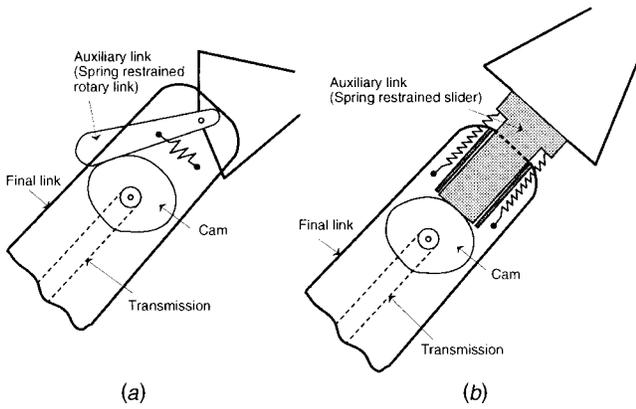
Fig. 6 Auxiliary links are mounted at the tip of the SDCSC mechanism: (a) Rotational and (b) Translational.

four-bar (with E as the coupler point) at the same first position and the dashed lines depict its other positions during the motion. Curves with greater changes in curvature can be traced in PF problems because the orientation matching requirement is absent as seen in Fig. 5(b).

4.3.1 Better End-Effector Position and Orientation Matching for RBG Tasks. SDCSC mechanisms can only realize end-effector orientations which are a linear function of the input crank angle. To accommodate other variations, we include a rotating auxiliary link to compensate for the discrepancies in orientations. The auxiliary link, depicted in Fig. 6(a) is pivoted at the curve tracing point of the Nth link, and the end-effector is aligned with the curve tracing point and rigidly attached to the auxiliary link. A cam, driven by the same cable-pulley arrangement, is used to provide the required compensatory motions of the auxiliary link, eliminating the need for an extra actuator. It is desirable to keep the compensatory rotations of the auxiliary rotating link small to simplify the cam design. A revised optimization scheme is developed [26] to simultaneously determine the optimal values for the parameters of the mechanism and the compensatory rotations. *Arbitrarily fine matching of the orientation can be achieved by designing the cam of the auxiliary link with a finer resolution after the optimization.*

4.3 Planar Kinematic Design Examples. An optimal 2-link SDCSC mechanism solution to the Rigid Body Guidance problem is illustrated in Fig. 5(a) for a typical feeding task discussed in the previous section. The solid line PQR depicts the 2-link SDCSC mechanism at the first precision point and the thin lines depict the mechanism through the various stages of the motion. For comparison, an optimal four-bar solution for the same dataset is superposed in the figure to demonstrate the relative sizes of the two configurations. ABCD denote the four joints of the

4.3.2 Better End-Effector Position Matching for PF Tasks In some situations, such as guiding the end-effector around the obstacles, matching the significant changes in the curvature tends to be beyond the geometric capability of the 2-link SDCSC
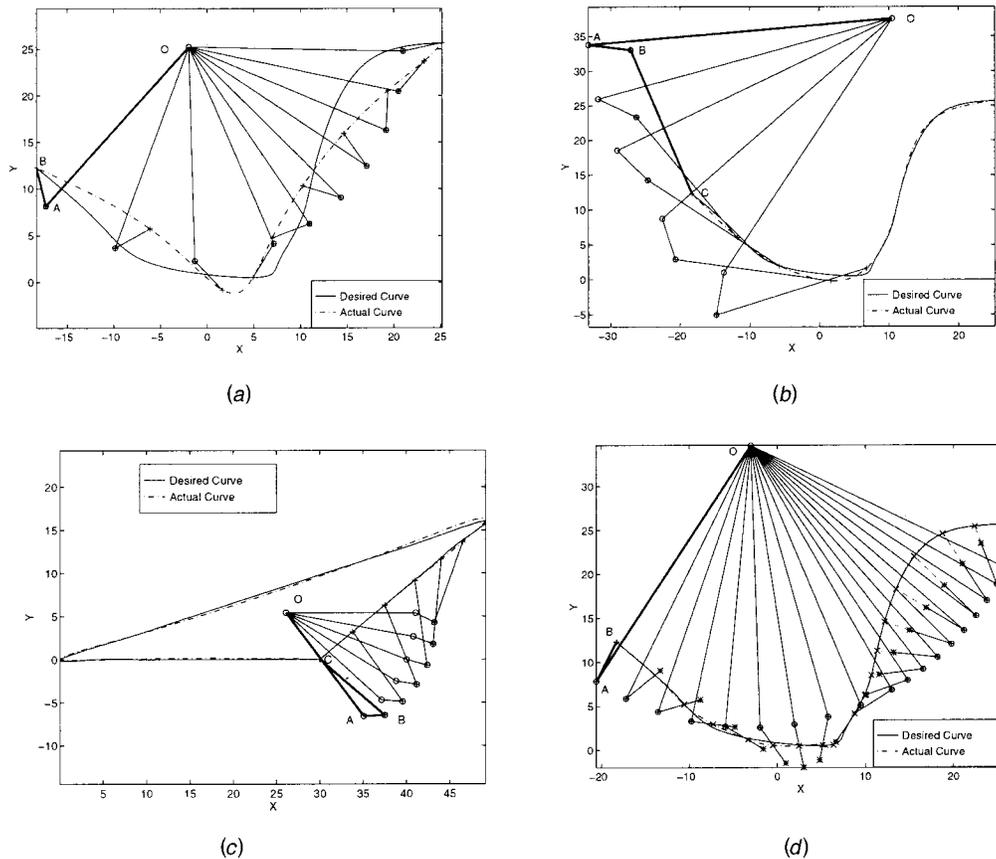

Fig. 7 Sample SDCSC mechanism solution for tracing a hand-drawn S shaped curve (a) 2-link and (b) 3-link. (c) A 3-link SDCSC mechanism solution for tracing a scalene triangle. (d) Fitting the hand drawn S shaped curve by a 2-link SDCSC mechanism equipped with a linear translational auxiliary link.
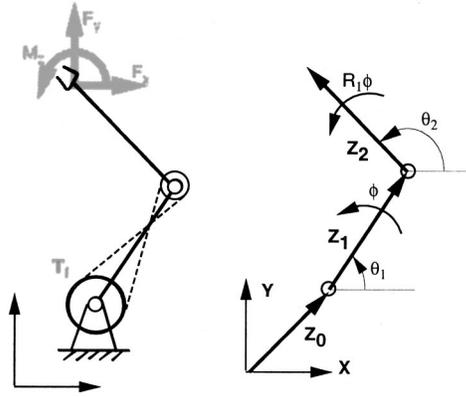
Fig. 8 Schematic of a 2-link single degree-of-freedom coupled serial chain (SDCSC) mechanism supporting an end-effector load using a single base actuator and its complex number vector representation.

mechanism, as shown in Fig. 7(a). Two options are explored to enhance the capabilities of the SDCSC mechanisms in such situations.

Increasing the number of links while retaining the single degree-of-freedom SDCSC configuration enhances the geometric curve tracing capability of the SDCSC mechanism. The improved tracing of the same hand-drawn curve with a three-link mechanism, while retaining a linear PPS procedure for 4 precision points, is shown in Fig. 7(b). The increased number of links also offers greater flexibility in tracing other complex curves such as the scalene triangle shown in Fig. 7(c).

As an alternative, we can consider adding a cam-driven axially extensible final link, shown in Fig. 7(b), driven by the input crank motion. A revised optimization problem is used to determine the dimensions of the optimal SDCSC mechanism, Fig. 7(d), to perform the task while keeping the required auxiliary translations small [26]. The auxiliary translation link can now provide *exact curve matching* since the cam can be designed appropriately after the mechanism synthesis.

5 Planar Kinetostatic Design and Optimization

Single degree-of-freedom mechanisms/linkages *can generate end-effector forces* only in directions tangential to the end-effector motion and structurally equilibrate forces in all other directions. Hence, we will explore the design of a mechanism to guide a rigid body while supporting *arbitrarily specified external loads*—by a combination of the structural equilibration and actuation— at each position along the trajectory.

5.1 Precision Point Synthesis. The force-measure precision point constraints are developed from the equations of static force-equilibrium for the 2-link SDCSC mechanism in this section and may be easily generalized to higher numbers of links. An input torque T_I is needed at the base joint to equilibrate an external load of $[F_x, F_y, M_z]^T$ applied at the end-effector, as shown in Fig. 8. By application of the principle of virtual work, we obtain:

$$F_x \delta Z_{Px} + F_y \delta Z_{Py} + M_z \delta \Theta + T_I \delta \phi = 0 \qquad (5)$$

Since this is a single degree-of-freedom mechanism, δZ_{Px}, δZ_{Py}, and $\delta \Theta$ are dependent on $\delta \phi$.

$$\begin{bmatrix} \delta Z_{Px} \\ \delta Z_{Py} \\ \delta \Theta \end{bmatrix} = \begin{bmatrix} -Z_{1x}S_\phi - Z_{1y}C_\phi - R_1 Z_{2x}S_{R_1\phi} - R_1 Z_{2y}C_{R_1\phi} \\ Z_{1x}C_\phi - Z_{1y}S_\phi + R_1 Z_{2x}C_{R_1\phi} - R_1 Z_{2y}S_{R_1\phi} \\ R_1 \end{bmatrix} \delta\phi \qquad (6)$$

where $C_\phi = cos(\phi)$, $S_\phi = sin(\phi)$, $C_{(\phi+\theta)} = cos(\phi+\theta)$ and $S_{(\phi+\theta)} = sin(\phi+\theta)$. Rearranging terms, we obtain a single scalar equation for the input torque as:

$$T_I(\phi) = -[A_1 \ A_2 \ A_3 \ A_4] \begin{bmatrix} Z_{1x} \\ Z_{1y} \\ Z_{2x} \\ Z_{2y} \end{bmatrix} - R_1 M_z \qquad (7)$$

$$A_1 = -F_x S_\phi + F_y C_\phi \qquad A_3 = R_1(-F_x S_{R_1\phi} + F_y C_{R_1\phi})$$

$$A_2 = -F_x C_\phi - F_y S_\phi \qquad A_4 = R_1(-F_x C_{R_1\phi} - F_y S_{R_1\phi})$$

An equivalent alternate expression for T_I may be obtained in terms of the link lengths by rearranging Eq. (7) as:

$$T_I(\phi) = -[B_1 B_2] \begin{bmatrix} L_1 \\ L_2 \end{bmatrix} - R_1 M_z \qquad (8)$$

$$B_1 = (-F_x S_{(\theta_1+\phi)} + F_y C_{(\theta_1+\phi)})$$

$$B_2 = R_1(-F_x S_{(\theta_2+R_1\phi)} + F_y C_{(\theta_2+R_1\phi)})$$

With the inclusion of torsional springs at the joints, the equation of virtual work needs to be modified to include the work done by the internal spring forces as shown below:

$$F_x \delta Z_{Px} + F_y \delta Z_{Py} + M_z \delta \Theta + T_I \delta \phi - K_1 \beta_1 \delta \beta_1 - K_2 \beta_2 \delta \beta_2 = 0 \qquad (9)$$

where β_1 and β_2 are the angular deflections of the torsional springs at the two joints.

$$\beta_1 = \theta_1 + \phi - \psi_1$$
$$\beta_2 = ((\theta_2 + R_1\phi - \psi_2) - (\theta_1 + \phi - \psi_1)) \qquad (10)$$

ψ_1 and ψ_2 are the absolute joint angles of the configuration of the mechanism where the undeflected springs are assembled whereas θ_1 and θ_2 correspond to the joint angles of the mechanism at its first precision point. Hence, the expression for the input torque, T_I, may now be written as:

$$T_I(\phi) = -[A_1 \ A_2 \ A_3 \ A_4] \begin{bmatrix} Z_{1x} \\ Z_{1y} \\ Z_{2x} \\ Z_{2y} \end{bmatrix} - R_1 M_z + K_1(\theta_1 + \phi - \psi_1)$$

$$+ K_2((\theta_2 - \theta_1) + (R_1 - 1)\phi - (\psi_2 - \psi_1))(R_1 - 1) \qquad (11)$$

The PPS constraints are now created by evaluating both the kinematic loop-closure and static force-equilibrium equations at the precision points and simultaneously solved in a *kinetostatic synthesis* approach to determine the dimensions of the mecha-

Table 2 Enumeration of free choices for a two-link SDCSC mechanism for the *PF* problem with *kinetostatic* specifications—without and with spring assists for $\Omega_i = \theta_i$ and $\Omega_i \neq \theta_i$ for various precision points

	Kinetostatic *No Springs*			Kinetostatic $\Omega_i = \theta_i$			Kinetostatic $\Omega_i \neq \theta_i$		
PP	Equations	Variables	Free Choices	Equations	Variables	Free Choices	Equations	Variables	Free Choices
M	$3M$	$Z_0, Z_1, Z_2, R_1,$ $\phi_2, \ldots, \phi_M$	$6 - 2M$	$3M$	$Z_0, Z_1, Z_2, R_1,$ $\kappa_1, \kappa_2, \Omega_1, \Omega_2,$ $\phi_2, \ldots, \phi_M$	$8 - 2M$	$3M$	$Z_0, Z_1, Z_2, R_1,$ $\kappa_1, \kappa_2, \Omega_1, \Omega_2,$ $\phi_2, \ldots, \phi_M$	$10 - 2M$
2	6	8	2	6	10	4	6	12	6
3	9	9	0	9	11	2	9	13	4
4	12	10	-	12	12	0	12	14	2
5	15	11	-	10	13	-	15	15	0

nism. Huang and Roth [20] note that combining the position and static-equilibrium constraints drastically limits the number of reachable precision points for the four-bar mechanism. This is also true for the 2-link SDCSC mechanism—see Table 2. Spring elements add extra design variables without adding design equations permitting the design for a slightly larger number of precision positions. Methods such as incomplete design specification [23] or mixed design specification [24] are also important here since they reduce the number of the design equations per precision point, permitting more precision points. For example, a *static synthesis* approach may be employed in situations where the position is irrelevant using only constraints on the *force measure* at precision points.

5.2 Planar Kinetostatic Design Examples

5.2.1 Example A: Peak Torque Minimization. In this example, a 2-link SDCSC mechanism is designed to match prescribed position and force specifications at two precision points exactly while minimizing the absolute value of the peak torques over the rest of the trajectory. In the feeder design case, the two precision points are selected to be at the beginning and end of the motion, the positions of the plate (-18.29 cm, 4.41 cm) and the mouth (25.19 cm, 25.19 cm). Further, we desire these to be positions of rest to be maintained without exerting any torque ($T_{I_1} = T_{I_2} = 0$). Finally, we will require the transition between positions to be accomplished using the smallest input-torques, while supporting a constant end-effector load ($F = [0, -1]^T N$). We examine the feasibility of achieving this goal without the use of springs (Case I) and later demonstrate the benefits of adding springs to lower the required input torques (Cases II and III).

Case I: Without Springs. The optimization problem may be stated as:

$$\min_{R_1, \phi_2} \quad \max_{\phi} |T(\phi)|$$

subject to:

$$\begin{bmatrix} X_{P_2} - X_{P_1} \\ Y_{P_2} - Y_{P_1} \\ T_{I_1} + R_1 M_{Z_1} \\ T_{I_2} + R_1 M_{Z_2} \end{bmatrix} = \begin{bmatrix} M_{11} & M_{12} & M_{13} & M_{14} \\ M_{21} & M_{22} & M_{23} & M_{24} \\ A_{11} & A_{12} & A_{13} & A_{14} \\ A_{21} & A_{22} & A_{23} & A_{24} \end{bmatrix} \begin{bmatrix} Z_{x1} \\ Z_{y1} \\ Z_{x2} \\ Z_{y2} \end{bmatrix}$$

where

$$M_{11} = (C_{\phi_2} - 1) \qquad M_{21} = S_{\phi_2}$$
$$M_{12} = -S_{\phi_2} \qquad M_{22} = (C_{\phi_2} - 1)$$
$$M_{13} = (C_{R_1 \phi_2} - 1) \qquad M_{23} = S_{R_1 \phi_2}$$
$$M_{14} = -S_{R_1 \phi_2} \qquad M_{24} = (C_{R_1 \phi_2} - 1)$$
$$A_{k1} = (F_{x_k} S_{\phi_k} - F_{y_k} C_{\phi_k}) \quad A_{k3} = R_1 (F_{x_k} S_{(R_1 \phi_k)} - F_{y_k} C_{R_1 \phi_k})$$
$$A_{k2} = (F_{x_k} C_{\phi_k} + F_{y_k} S_{\phi_k}) \quad A_{k4} = R_1 (F_{x_k} C_{R_1 \phi_k} + F_{y_k} S_{R_1 \phi_k})$$

$$(12)$$

The first two scalar equations represent the kinematic constraints while the remaining two are the force-measure constraints at the two precision points. The selection of R_1 and ϕ_2 as free choices yields a strongly coupled system (in the kinematic and force-measure equations) but makes the solution of the system of equations linearly for the remaining unknowns $Z_{x1}, Z_{y1}, Z_{x2}, Z_{y2}$ possible.

Spring assists alter the desired input torques via the equation of virtual work, adding new variables – Ω_i, the absolute joint configuration when springs are attached; and κ_i the spring constants—but do not add other new equations. Two further cases result when the springs are added and are discussed next.

Case II: Springs Assembled at the Initial Configuration ($\Omega_i = \theta_i$). The first case is one where the undeflected position of the springs occurs when the end effector is at the first precision point. Such an assumption is useful in a practical setting since the mounting of the springs can be guaranteed at the first precision point. Thus $\Omega_i = \theta_i$ which considerably simplifies the expression for the contribution to the input torques:
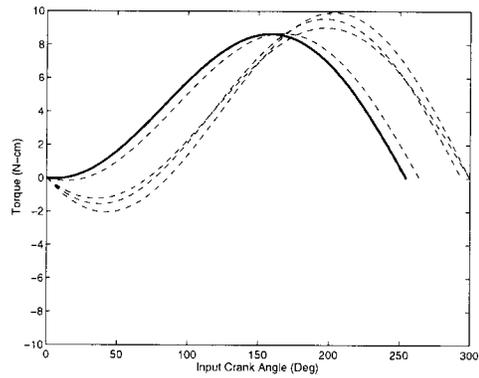
$$T_{Spring}(\phi) = -\kappa_1 \phi - \kappa_2 (R_1 - 1)^2 \phi \qquad (13)$$

$$T_{Input} = T_{Equil} - T_{Spring}$$

The new variables κ_1 and κ_2 increase the total number of variables by two. We continue to treat the two-precision point case employing an increased number of free choices, ϕ_2, R_1, κ_1 and
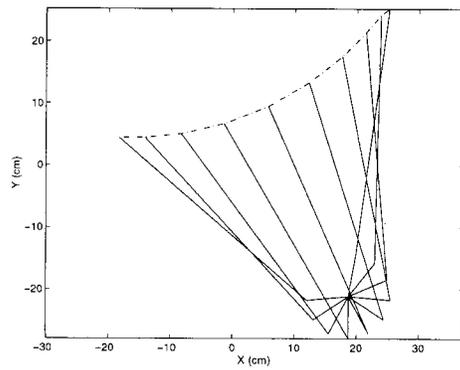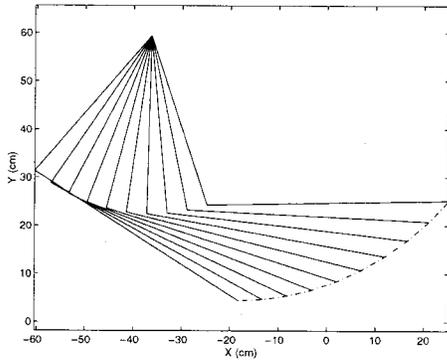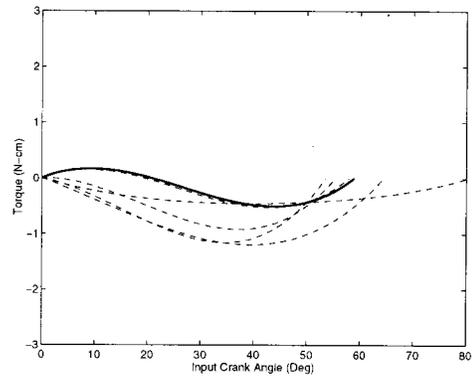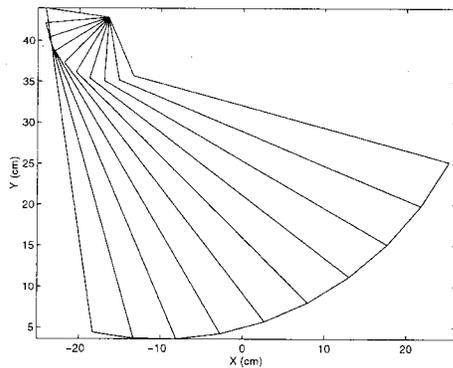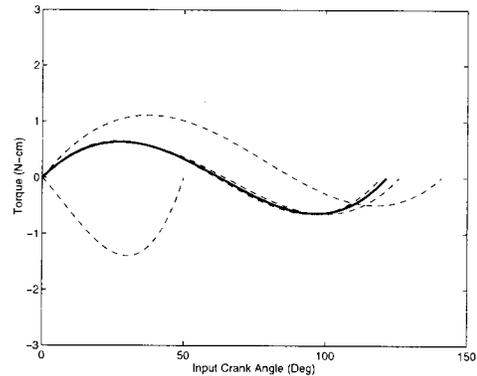
Fig. 9 Two precision point kinetostatic synthesis combined with minimization of the maximum absolute torque. Cases (I) Without Spring Assist (II) With Undeflected Springs Assembled at the Initial Configuration; and (III) With Undeflected Springs Assembled at a General Configuration. Figures (a) (c) and (e) depict the optimal mechanism moving between the start and end points. Figures (b), (d) and (f) show intermediate input-torque profiles converging to the optimal (solid line) profile. All the torque profiles satisfy the prescribed zero input-torque requirements at the start and finish.

κ_2, leading to a strongly coupled system of linear equations which may be solved for the remaining unknowns Z_{x1}, Z_{y1}, Z_{x2}, Z_{y2}. The optimization problem may be stated as:

$$\min_{R_1,\phi_2,\kappa_1,\kappa_2} \quad \max_{\phi}|T(\phi)|$$

subject to:

$$\begin{bmatrix} X_{P_2}-X_{P_1} \\ Y_{P_2}-Y_{P_1} \\ T_{I_1}-T_{S_1}+R_1 M_{Z_1} \\ T_{I_2}-T_{S_2}+R_1 M_{Z_2} \end{bmatrix} = \begin{bmatrix} M_{11} & M_{12} & M_{13} & M_{14} \\ M_{21} & M_{22} & M_{23} & M_{24} \\ A_{11} & A_{12} & A_{13} & A_{14} \\ A_{21} & A_{22} & A_{23} & A_{24} \end{bmatrix} \begin{bmatrix} Z_{x1} \\ Z_{y1} \\ Z_{x2} \\ Z_{y2} \end{bmatrix}$$

Journal of Mechanical Design

JUNE 2002, Vol. 124 **/ 309**

where

$$M_{11}=(C_{\phi_2}-1) \qquad M_{21}=S_{\phi_2}$$

$$M_{12}=-S_{\phi_2} \qquad M_{22}=(C_{\phi_2}-1)$$

$$M_{13}=(C_{R_1\phi_2}-1) \qquad M_{23}=S_{R_1\phi_2}$$

$$M_{14}=-S_{R_1\phi_2} \qquad M_{24}=(C_{R_1\phi_2}-1)$$

$$A_{k1}=(F_{x_k}S_{\phi_k}-F_{y_k}C_{\phi_k}) \quad A_{k3}=R_1(F_{x_k}S_{R_1\phi_k}-F_{y_k}C_{R_1\phi_k})$$

$$A_{k2}=(F_{x_k}C_{\phi_k}+F_{y_k}S_{\phi_k}) \quad A_{k4}=R_1(F_{x_k}C_{R_1\phi_k}+F_{y_k}S_{R_1\phi_k})$$

$$T_{S_1}=0 \qquad T_{S_2}=-\kappa_1\phi_2-\kappa_2(R_1-1)^2\phi_2$$

$$(14)$$

Case III: Springs Assembled at a General Configuration ($\Omega_i\neq\theta_i$). In many cases, we would like all precision points to be ''load-bearing.'' Hence, we assemble the springs at positions away from the precision points so as to preload the mechanism at the configurations reached at the precision points ($\Omega_i\neq\theta_i$). Note that the constraints written using Cartesian link coordinates are not as useful here. In their stead, we express all the constraints (kinematic and static) in terms of the magnitudes of the link lengths. In recasting the equations, the system of equations is linear in terms of the magnitudes of various link lengths which are now selected to be the dependent parameters. The spring constants are selected as the other dependent parameters. The combined system may be written in matrix form as seen in the constraints of Eq. (15). The 6 available free choices are used to specify ϕ_2, R_1, θ_1, θ_2, Ω_1, Ω_2 which leads to a weakly coupled system of linear equations [4] which may be solved for the dependent variables L_1, L_2, κ_1, κ_2.

The weak coupling implies that the kinematic equations may first be solved independently for a few of the variables L_1, L_2. These results are then used to solve the static equations for the remaining unknowns κ_1, κ_2. We will, however, prefer to solve the combined system of equations and perform the optimization on the entire set of variables simultaneously. Note that care must also be taken to ensure non-negative values for the dependent variables in this case.

$$\min_{R_1,\phi_2,\theta_1,\theta_2,\Omega_1,\Omega_2}\quad \max_{\phi}|T(\phi)| \qquad (15)$$

subject to:

$$\begin{bmatrix} X_{P_2}-X_{P_1} \\ Y_{P_2}-Y_{P_1} \\ T_{I_1}+R_1M_{z_1} \\ T_{I_2}+R_1M_{z_2} \end{bmatrix} = \begin{bmatrix} M_{11} & M_{12} & 0 & 0 \\ M_{21} & M_{22} & 0 & 0 \\ A_{11} & A_{12} & A_{13} & A_{14} \\ A_{21} & A_{22} & A_{23} & A_{24} \end{bmatrix} \begin{bmatrix} L_1 \\ L_2 \\ \kappa_1 \\ \kappa_2 \end{bmatrix}$$

where

$$M_{11}=C_{(\theta_1+\phi_2)}-C_{\theta_1} \qquad A_{11}=(F_{x_1}S_{\theta_1}-F_{y_1}C_{\theta_1})$$

$$M_{12}=C_{(\theta_2+R_1\phi_2)}-C_{\theta_2} \qquad A_{12}=R_1(F_{x_1}S_{\theta_2}-F_{y_1}C_{\theta_2})$$

$$M_{21}=S_{(\theta_1+\phi_2)}-S_{\theta_1} \qquad A_{21}=F_{x_2}S_{(\theta_1+\phi_2)}-F_{y_2}C_{(\theta_1+\phi_2)}$$

$$M_{22}=S_{(\theta_2+R_1\phi_2)}-S_{\theta_2} \qquad A_{22}=R_1F_{x_2}S_{(\theta_2+R_1\phi_2)}$$

$$\qquad\qquad\qquad\qquad\qquad -R_1F_{y_2}C_{(\theta_2+R_1\phi_2)}$$

$$D_{11}=(\theta_1-\Omega_1) \qquad D_{21}=(\theta_1+\phi_2-\Omega_1)$$

$$D_{12}=(\theta_2-\Omega_2) \qquad D_{22}=(\theta_2+R_1\phi_2-\Omega_2)$$

$$\qquad -(\theta_1-\Omega_1) \qquad\qquad -(\theta_1+\phi_2-\Omega_1) \qquad (15)$$

Discussion. In our experience with several examples, we did not experience any difficulty with the min-max formulation, possibly because the precision point equations lead the optimization to the portion of the design space where the non-differentiability is not a problem. However, we note that it is possible to recast the above min-max problem easily as a constrained minimization problem by introducing an additional slack variable and several additional inequality constraints, a technique commonly used in structural optimization.

The results of the optimization over the free choices in each of the three cases are depicted each of the three rows of Fig. 9. In each of the figures on the left hand side, (a), (c), and (e), the obtained mechanism solution is depicted moving between the start and end points, which were selected to be the precision points. In the figures on the right, (b), (d), and (f), the several intermediate input torque profiles (dashed lines) are shown converging to the optimal (solid line) profile. The final profile (solid curve) has the lowest absolute value of the peak torque among all other curves. Note that all the position profiles interpolate the start and finish points and that the torque profiles satisfy the prescribed zero input-torque requirements at these positions. Comparing the figures on the right, (b), (d), and (f), we would like to emphasize the *reduction* in the required torques in Cases II and III by *an order of magnitude* due to the addition of spring assists.

5.2.2 Example B: Position-Independent Input Torque Profile Matching. Four-bar linkages have been used in the design of exercise machines to give their users a shaped exercise profile using a constant load/weight [3]. In this example, we will demonstrate the distinct benefits of using a 2-link SDCSC mechanism supporting a constant end-effector weight, instead of a four-bar linkage. The user interacts primarily only with the input handle attached to the rotation of the base joint and so the motion (position profile) of the end-effector is not relevant. Hence a wide variety of desired shaped input torque profiles can be realized by: (a) eliminating the dependence on the positions from the objective; and (b) supplanting the constraints on the end-effector position with further design specifications on the input torques. This increase in the number of torque specifications enhances the optimization process by reducing the feasible search space resulting in a more rapid convergence. Representative results of the design of mechanisms which use the shaped quadratic and cubic shaped input torque profile to support the constant load at the end-effector are presented here in Fig. 10 and discussed further in [26].

6 Conclusion

In this paper, we introduced a novel configuration of mechanisms called Single Degree-of-freedom Coupled Serial Chain (SDCSC) mechanisms and presented a general framework and methodology for their synthesis for planar tasks. A salient feature
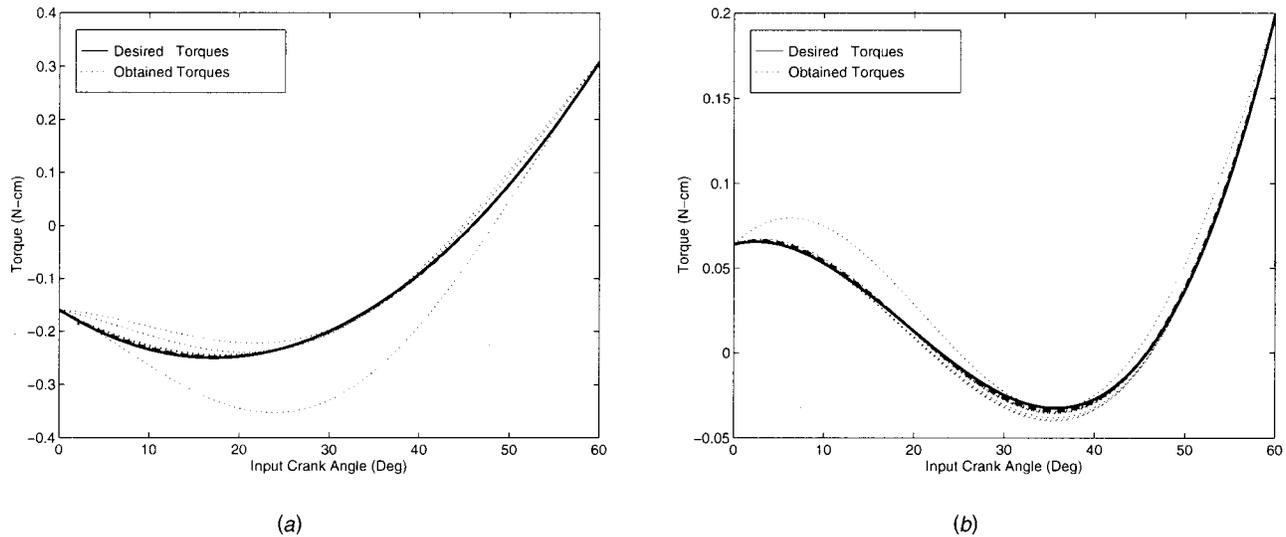
Fig. 10 Desired input torque profile matching (*a*) Quadratic Profile $T(\phi_N)=\phi_N^2-0.6\phi_N-0.16$ and (*b*) Cubic Profile $T(\phi_N)=\phi_N^3 -\phi_N^2+0.08\phi_N+0.064$ where $\phi_N=(\phi/60)$. The final designed mechanism is required to support an applied load of $F=[0,-1]^T N$ at the end effector using the desired input torque profile (solid line). The intermediate non-optimal torque profiles are shown in dotted lines converging to the final optimal profile shown in dashed (− −) line.

of the SDCSC mechanism is the constant angular velocity ratio between the end-effector link and the drive link imposed by the coupling pulleys. This plays a significant role in the creation and easy solution of the precision point constraints.

The developed framework allows the designer to specify an end-effector trajectory and prescribe forces along it and to match the kinematic and kinetostatic specifications exactly at the precision points and in a least squares sense over the entire range. The framework permits tradeoff between exact and approximate matching of specifications, such as by selecting the number, location of precision points and the relative weighting. Further, a new correspondence measure called "equal arc-length segment correspondence" was developed and successfully used in optimization.

The kinetostatic design methodology detailed in this paper is a combination of kinematic design, structural equilibration design and design with spring assists, which permits the designer to arrive at optimal values for the mechanism parameters as well as the spring parameters simultaneously. The addition of springs substantially reduces the input torque requirements as demonstrated in the examples. Once designed and fabricated such SDCSC mechanisms can only realize a particular motion/force profile at its end-effector and cannot be reconfigured to other tasks easily. Currently care must be taken while designing the mechanisms to be able to satisfy selected design specifications. However, the reduced costs of manufacture and operation of such mechanisms would be instrumental in overcoming any disadvantages created by the loss of flexibility of reconfiguration to a new task. The reintroduction of flexibility of reconfiguration by varying the mechanical constraints is being addressed in ongoing work.

Examples were presented to highlight each of the methods described in the paper. In the examples considered we explored the suitability of using such SDCSC mechanisms for conventional manipulation tasks — examining the benefits, the limitations and proposing methods to overcome these limitations. These examples suggest that multi-link single degree-of-freedom coupled serial chain mechanisms may help fill the gap between the versatile but expensive multi-degree-of-freedom, computer-controlled robots and the relatively bulky but inexpensive single degree-of-freedom closed-loop linkages.

References

[1] Krovi, V., Kumar, V., Ananthasuresh, G. K., and Vezien, J.-M., 1999, "Design and Virtual Prototyping of Rehabilitation Aids," ASME J. Mech. Des., **121**(3), pp. 456–458.

[2] Nie, X., and Krovi, V., 2001, "Design of Passive Reconfigurable Manipulation Assistive Aids," Proceedings of the 2001 ASME Design Engineering Technical Conferences, Paper No. DETC2001/DAC-21087, Pittsburgh, PA.

[3] Scardina, M. T., Soper, R. R., Calkins, J. M., and Reinholtz, C., 1995, "Optimal Synthesis of Force Generating Planar Four-link Mechanisms," Proceedings of the 4th National Applied Mechanisms and Robotics Conference, Paper No. AMR 95-003, Cincinnati, OH.

[4] Howell, L. L., and Midha, A., 1996, "A Loop Closure Theory for the Analysis and Synthesis of Compliant Mechanisms," ASME J. Mech. Des., **118**, No. 1, pp. 121–126.

[5] Chirikjian, G. S., and Burdick, J. W., 1994, "A Model Approach to Hyperredundant Manipulator Kinematics," IEEE Trans. Rob. Autom., **10**, No. 3, pp. 343–354.

[6] Hunt, K., 1978, *Kinematic Geometry of Mechanisms*, Clarendon Press, Oxford.

[7] Freudenstein, F., and Primrose, E., 1963, "Geared Five-bar Motion, Part 1—Gear Ratio Minus 1," ASME J. Appl. Mech., **85**, No. E, pp. 161–169.

[8] Sandor, G. N., 1964, "On the Existence of a Cycloidal Burmester Theory in Planar Kinematics," ASME J. Appl. Mech., **86**, No. E, pp. 694–699.

[9] Kaufman, R. E., and Sandor, G. N., 1969, "Bicycloidal Crank—A New Four-link Mechanism," ASME J. Eng. Ind., **91**, No. B, pp. 91–96.

[10] Tsai, L.-W., 1995, "Design of Tendon-driven Manipulators," ASME J. Mech. Des., **117**, No. 2B, pp. 80–86.

[11] Hirose, S., and Umetani, Y., 1978, "The Development of the Soft Gripper for the Versatile Robot Hand," Mech. Mach. Theory, **13**, pp. 351–359.

[12] Ma, S., Hirose, S., and Yoshinada, H., 1993, "Design and Experiments for a Coupled Tendon-Driven Manipulator," IEEE Trans. Control Syst. Technol., **13**, No. 1, pp. 30–36.

[13] Rosheim, M., 1997, "In the Footsteps of Leonardo," IEEE Rob. Autom. Mag., **4**, No. 2, pp. 12–14.

[14] Leaver, S., McCarthy, J. M., and Bobrow, J., 1988, "The Design and Control of a Robot Finger for Tactile Sensing," J. Rob. Syst., **5**, No. 6, pp. 567–581.

[15] Figliolini, G., and Ceccarelli, M., 1998, "A Motion Analysis for One-d.o.f. Anthropomorphic Finger Mechanism," Proceedings of the 1998 ASME Design Engineering Technical Conferences, Paper No. DETC98/MECH-5985, (Atlanta, GA).

[16] Sandor G. N., and Erdman, A. G., 1984, *Advanced Mechanism Design: Analysis and Synthesis*, **2**, Prentice Hall International, Englewood Cliffs, NJ.

[17] Bagci, C., 1987, "Synthesis of Linkages to Generate Specified Histories of Forces and Torques: Part 1—The Planar Four-bar Mechanism," Advances in Design Automation, 13th ASME Design Automation Conference (S. Rao, ed.), DE-Vol. 10-2, pp. 227–236.

[18] Matthew, G. K., and Tesar, D., 1977, "Synthesis of Spring Parameters to Balance General Forcing Functions in Planar Mechanisms," ASME J. Eng. Ind., **99**, pp. 347–352.

[19] Idlani, S., Streit, D. A., and Gilmore, B. J., 1993, ''Elastic Potential Synthesis—A Generalized Procedure for Dynamic Synthesis of Machine and Mechanism Systems,'' ASME J. Mech. Des., **115**, No. 3, pp. 568–575.

[20] Huang, C., and Roth, B., 1993, ''Dimensional Synthesis of Closed-loop Linkages to Match Force and Position Specifications,'' ASME J. Mech. Des., **115**, No. 2, pp. 194–198.

[21] Sarkisyan, Y. L., Gupta, K. C., and Roth, B., 1973, ''Kinematic Geometry Associated with the Least Square Approximation of a Given Motion,'' ASME J. Eng. Ind., **95**, pp. 503–510.

[22] Kramer, S. N., *Selective Precision Synthesis of Planar Mechanisms Satisfying Practical Design Requirements*, Ph.D. thesis, Rennsalear Polytechnic Institute, Troy, NY.

[23] Tsai, L.-W., and Roth, B., 1973, ''Incompletely Specified Displacements: Geometry and Spatial Linkage Synthesis,'' ASME J. Eng. Ind., **95**, pp. 603–611.

[24] Chuang, J. C., and Waldron, K. J., 1983, ''Synthesis with Mixed Motion and Path Generation Position Specifications,'' ASME J. Mech., Transm., Autom. Des., **105**, No. 4, pp. 617–624.

[25] Akhras, R., and Angeles, J., 1990, ''Unconstrained Nonlinear Least-squares Optimization of Planar Linkages for Rigid-body Guidance,'' Mech. Mach. Theory, **25**, pp. 97–118.

[26] Krovi, V., 1998, *Design and Virtual Prototyping of User-Customized Assistive Devices*, Ph.D. thesis, Mechanical Engineering and Applied Mechanics, University of Pennsylvania.